X-Transport as a Basic Source of Edge Pedestal and H-Mode in a Diverted Tokamak

C.S. Chang 1)2), D. Darrow 3), S.H. Ku 2), H. Weitzner 1), R. White 3), Z. Lin 3), W. Lee 3), T. Carlstrom 4), J. deGrassie 4)

1) Courant Institute of Mathematical Sciences, New York University, 251 Mercer St., New York, N.Y. 10012, USA.
2) Department of Physics, KAIST, Taejon, Korea
3) Princeton Plasma Physics Laboratory, Princeton, NJ 08543, USA
4) General Atomics, P.O. Box 85608, San Diego, CA 92186, USA

e-mail contact of main author: cschang@cims.nyu.edu

Abstract. A new classical non-ambipolar transport mechanism has been identified which can be a dominant source of strong Er and edge pedestal layer formation immediately inside the separatrix in a diverted tokamak. Due to vanishingly small poloidal B-field and grad-B drift toward x-point, plasma ions with small $v_{||}$ in the X-region do not have confined single particle orbits. This leads to a non-ambipolar convective transport in the X-region (X-transport), either collisional or collisionless, inducing a strong negative Er-shear layer. The X-transport can provide basic understanding of many of the experimental observations.

Experiments suggested that a H-mode transition prefers ∇B drift into a divertor, that a double null geometry raises the H-mode power threshold over that of a single null, that there is usually an edge pedestal formation in a diverted plasma regardless of the operation mode (weaker in L-mode), and that the effective collisionality ν_* is not a critical parameter for an H-mode transition. Numerous neoclassical and turbulence theories have emerged trying to understand these phenomena. However, it has been realized recently by one of the authors[1] that perhaps the most dominant non-ambipolar mechanism in the plasma edge is the non-tokamak type transport near the divertor X-point, from which the above observations are natural consequences.

For single particle confinement in an axisymmetric tokamak where the particle motion is subject to ∇B drift, it is necessary to have a reasonably large poloidal magnetic field B_p: The plasma transport is then automatically ambipolar. However, in the plasma near the divertor X-point (X-region), B_p becomes vanishingly small and unconfined single particle orbits appear. Ions in the X-region with small parallel speed will have little poloidal speed to escape out of this region and they get poloidally trapped (X-trapping). They are subject to vertical ∇B-drift motion one way out of the plasma, across the last closed flux surface into the divertor chamber. The electron parallel motion is still much faster than the ∇B drift motion and, thus, their poloidal X-trapping effect is negligible. This can lead to a preferential loss of ions into the divertor region and, thus, to a strongly negative ambipolar radial electric field immediately inside of the separatrix.

Figure 1 shows a typical unconfined collisionless ion orbit in the X-region of DIII-D, evaluated using a collisionless Lorentz particle orbit code. Figure 2 shows the unconfined region in the D ion distribution function at 10 cm above the X-point. The vertical and horizontal axes represent perpendicular and parallel speeds, given as the square-root of the perpendicular and parallel energy in keV, respectively. The flux surface at 10 cm above the X-point corresponds to 0.5 cm inside of the separatrix surface at the outside midplane. It can be seen from Fig. 2 that the orbit loss extends all the way down to 80 eV, which is about or below the ion thermal energy at the observation point.

This leads to a non-ambipolar loss of plasma ions even at the thermal level in the X-region.

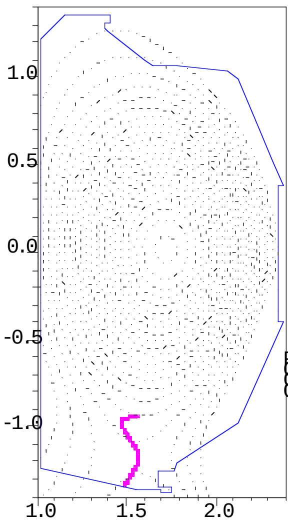

Fig. 1. Unconfined ion orbit by X-trapping in DIII-D.

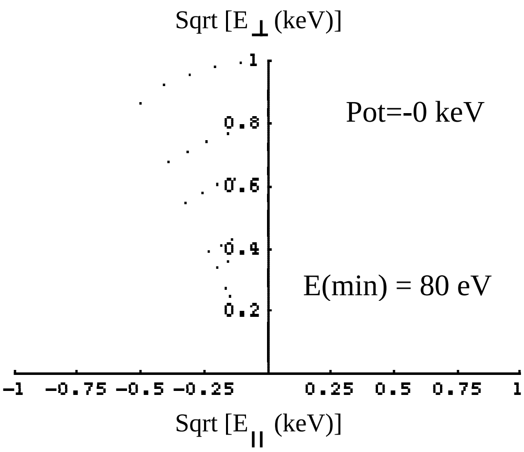

Fig. 2. Ion velocity space hole at 10 cm above the X-point in DIII-D.

In fact, the plasma ions in the narrow loss region at the thermal energy are not subject to direct orbit loss, but to collisional transport loss, since they suffer pitch angle collisions before they ∇B-drift to the separatrix surface. The collisional convective transport speed of thermal ions induced by the existence of a loss hole of the size $\Delta\xi \sim 0.1$ and vertical drift speed $V_{\nabla B}$ can easily be evaluated to be $\sim 10^{-1}$ m/s for the loss orbit configuration as shown in Fig. 2 under a DIII-D plasma edge condition. Such a non-ambipolar transport cannot be allowed by the plasma and an electrostatic potential well develops to shift the loss hole to a higher energy, where the equilibrium ambipolar electric field is influenced by the weakly collisional higher energy ions, which can drift across most of the X-region without scattering out of the loss hole. Some of the unconfined ions near the left boundary travel a long way to toward maximal B-field side and bounce back to get lost in the X-region. These ions, at any reasonable energy, do not participate in the weakly collisional X-loss process due to their high effective pitch angle scattering rate. The magnitude of the collisional and collisionless ion loss must be reduced to the level of the neoclassical return current to keep the plasma quasineutral. An ambipolar negative electric field will reduce the X-loss current J_x and increase the return current J_{ret}. The electric field strength grows until the ambipolarity $J_x(E_r)+J_{ret}(E_r) = 0$ is satisfied.

The loss region in v-space is not empty. When mapped to the poloidal angle θ away from the X-region ($\theta \neq \theta_x$) the loss region in pitch angle space becomes much narrower, raising the effective pitch angle scattering rate ν_{x*}. Figure 3 shows the loss region of Fig. 2 mapped to the outside midplane. ν_{x*} value during their poloidal motion at $\theta \neq \theta_x$ is greater than unity for any reasonably high energy ions which are relevant to this process. Thus, the velocity space region is rapidly filled at $\theta \neq \theta_x$ by collisions, being at a collisional equilibrium with the rest of the distribution function. The lost tail ions at the X-region are re-supplied by the in-flow of high energy ions from other poloidal angle, by pitch angle scattering from within the X-region (at lower energy), and by the neutral

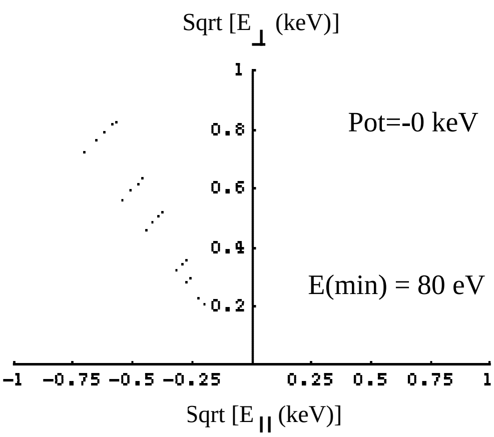

Fig. 3. Ion velocity space hole mapped to 0.5 cm inside of the separatrix at midplane in DIII-D.

ionization in the X-region: the ion density in the loss hole at the X-region should not be much lower than that of its environment. An adequate number of local neutrals in the X-region can help enhance the X-loss by raising the ion density in the loss hole, as long as there are not so many of them to keep the edge T_i too low.

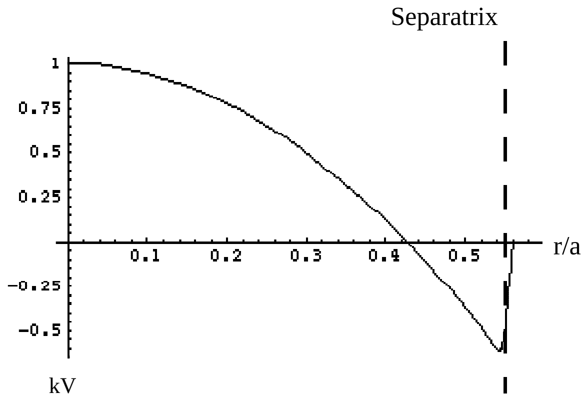

Fig. 4. Potential profile Model

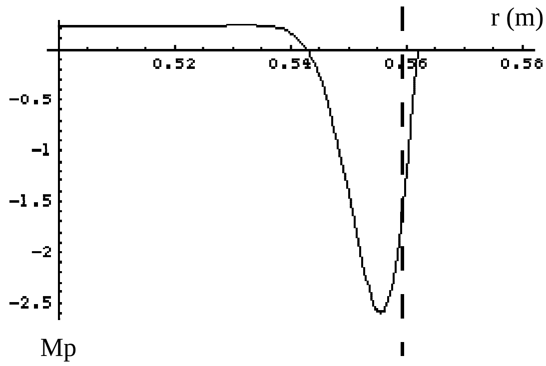

Fig. 5. Poloidal ExB speed Mach number Mp

The X-loss current has been determined numerically on several flux surfaces for several different radial electric field values, from which an analytic fit has been generated to obtain a formula for the X-loss current (X-current) as a function of radial electric field, ion temperature, and ion density in a DIII-D flux equilibrium as given in Fig. 1. For the electrostatic potential profile shape a model has been adopted (see Figs. 4 and 5 which describes a H-mode situation), which has a parabolic shape followed by a sharp exponential drop in the X-loss region. The depth of the edge potential and width of the large E_r layer have been adjusted to approximately reduce the ion X-current to the ambipolar level at every distance above the X-point for a given edge T_i profile, using an analytic neoclassical viscosity formula $J_{ret} =< \nabla \cdot \mathbf{\Pi} >_\theta /B_t$ for the return current.

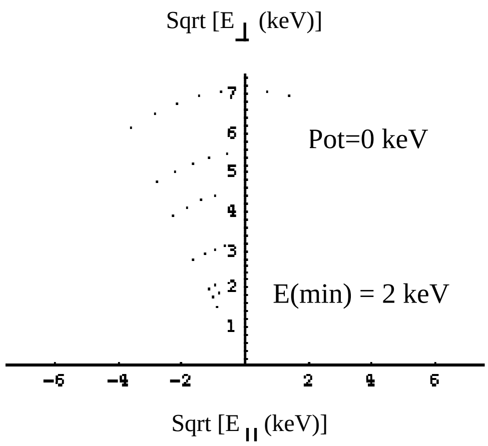

Fig. 6. Ion velocity space hole for 0 keV potential in DIII-D at R=156 cm, DZ=23 cm.

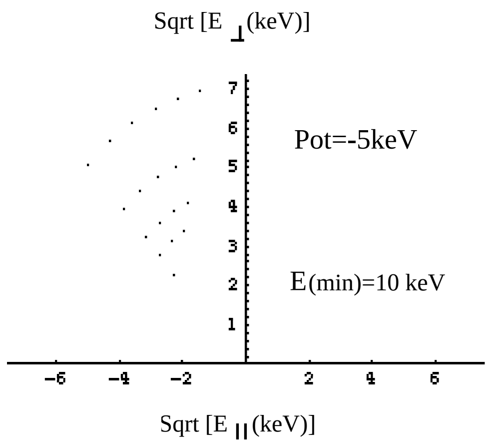

Fig. 7. Ion velocity space hole for -5 keV potential depth in DIII-D at R=156 cm, DZ=23 cm.

Tanh type of n_e and T_i profiles is used with $n_e = 1 \times 10^{13}\text{cm}^{-3}$, $T_i = 300$ eV at the inversion point. An initial guess for a common width for density and temperature profiles is eventually converged to be consistent with the E_r layer width. The maximal electric field occurs at $\Delta_{\max} = 0.7$ cm inside of the separatrix at the outside midplane, where the inversion point of the tanh n_e and T_i profiles is eventually adjusted to be.

At flux surfaces where the X-current is small, accuracy of the model is not emphasized. For example, at 23 cm above the X-point (corresponding to 2.5 cm on the midplane), a weak ambipolar electric field is assumed without demanding accuracy. The width of the strong E_r layer can be estimated as $2\Delta_{\max} = 1.4\ cm$, which is close to an experimental observation. Figure 7 shows a demonstration of the up-shifted loss hole in energy when an electric potential depth of -5 keV is introduced to the case of Fig. 6. The minimum loss energy has been shifted from 2 keV to 10 keV. Note here that the loss hole is also shifted in the pitch angle direction due to the $E \times B$ effect.

In determining the ambipolar electric field from the ambipolarity equation $-J_x = J_{ret} =< \nabla \cdot \mathbf{\Pi} >_\theta /B_t$, which is identical to the neoclassical poloidal force balance equation, there are a couple of uncertainties. One comes from the purely neoclassical nature of the present model, which neglects an anomalous electron loss. Inclusion of any anomalous electron loss should reduce the potential well depth. Another uncertainty arises from the difference between the poloidal $E \times B$ speed, $V_E = -E_r/B_t$, and the poloidal fluid speed, $V_p = V_E + (\nabla_r P + V_t B_p)/B_t$. Normally the poloidal flows from $\nabla_r P$ and V_t are developed in the opposite direction to V_E, making $V_p = kV_E$ with $k < 1$. If $J_x = 0$, it is well known that $k \ll 1$. In the above analysis, it has simply been assumed that $V_t \simeq 0$ in the plasma edge and $V_E \gg \nabla_r P/B_t$; thus, $k \simeq 1$. A more accurate analysis should evaluate $\nabla_r P$ from a transport equation. The $k \simeq 1$ assumption can be better justified right after a fast L to H transition before a transport process takes place: i.e., when a large V_E is established from a bifurcation, but $\nabla_r P$ is not yet steepened to reflect the transport reduction due to a large sheared $E \times B$ flow.

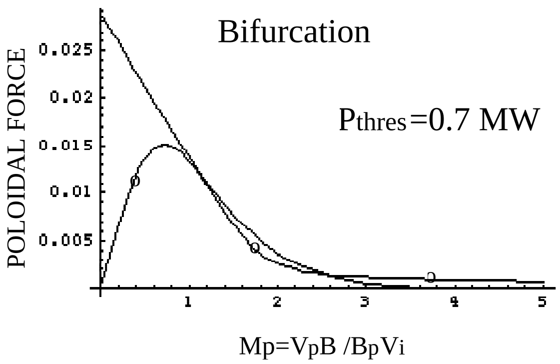

Fig. 8. Bifurcation from Mp=1.2 to 2.6. Plain line is the JxB force and circled line is the viscous force.

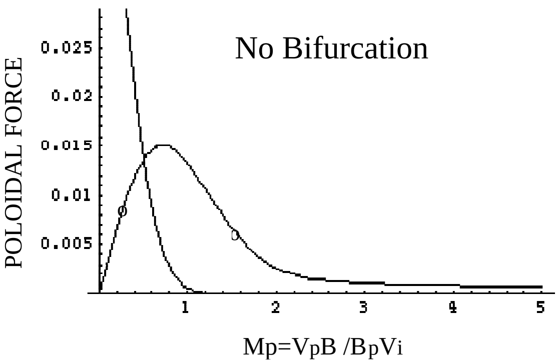

Fig. 9. Poloidal force balance equations indicating a gradual increase of VE = Vp/k with k =3.

It is found that a sudden bifurcation to a greater poloidal flow solution does not always exist in the neoclassical poloidal force balance equation. As the edge T_i is raised, J_x is increased. Under the assumption of $V_p = V_E$, the neoclassical equilibrium solution E_r gets stronger until it jumps to a bifurcated solution of Shaing's type[2] as can be seen from Fig. 8. However, if V_p is smaller than V_E, the decrease of J_x curve in V_p can be too fast to allow for multiple solutions (see Fig. 9). In this case, the $E \times B$ speed can become large without requiring the poloidal fluid speed to be large and a gradual transition to a critical E_r-profile for a turbulence suppression can be possible. An important factor in determining whether the H-transition is of bifurcation type or gradual type may be the relative time scale for the J_r increase compared to that for the local transport process. If the power flow into the X-region is fast enough, then J_x can rapidly increase before $|\nabla P|$ has time to respond. In this case V_p is not much smaller than V_E and the transition may be of bifurcation type (Fig. 8): The steepening of $|\nabla P|$ and relaxation of V_p can occur after the bifurcation. On the other hand, if the power flow into the X-region cannot support a rapid rise of J_x, the J_x increase rate can be as slow as the local transport time scale. $|\nabla P|$ can then develop to reduce $V_p \ll V_E$. In this case a gradual H-transition is possible (Fig. 9). We note here that the entire process considered here is not sensitive to the background ion collisionality ν_{*i}.

A recent experiment on DIII-D found that the H-mode transition is easier if the X-point is moved radially outward [3]. Fig. 10 shows the unconfined orbit region in v-space at 10 cm above the X-point at $R_x = 141$ cm and 156 cm. At 141 cm, the plasma is in L-mode, and at 156 cm, it is in H-mode [3]. It can be seen that the X-loss occurs at lower energy (60 eV) for larger $R_x = 156cm$ than 70 eV for 141 cm, which should yield a stronger X-loss at $R_x = 156cm$, thus easier H-transition.

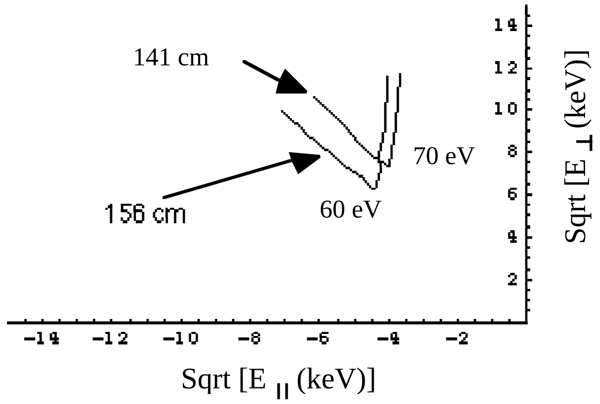

Fig. 10. Comparison between Rx=156 and 141 cm in DIII-D; DZ=10 cm, Pot=0 keV.

In conclusion, it has been shown that the radial electrical current generated by X-transport mechanism is significant enough to generate a strong E_r layer and H-mode transition. The E_r layer width from the X-loss is roughly consistent with the experimental pedestal width in DIII-D. However, the pedestal height may be determined from turbulence suppression and MHD phenomenon. Many of the experimental H-mode observations can be understood from the X-transport as natural phenomena, which includes the importance of the ∇B-drift into X-point in lowering the H-threshold, preference of single null over double null, existence of a (weak) pedestal even in an L-mode edge, insensitiveness to ν_{*i}, dependence on R_x, etc. We note here that a recent Monte Carlo guiding center orbit simulation within the separatrix in Ref. [4] partially supports the present argument by showing that a collisional edge particle transport requires a strong edge electric field for a net zero ion transport. Due to the pure numerical nature and restricted model used in the simulation, Ref. [4] was not able to discuss the detailed and convincing phase space mechanisms presented in the present work, nor it found a reasonable E_r-layer width or H-mode bifurcation. Reference [5] studied ion loss holes at the outside midplane in a diverted geometry, however, whithout realizing that there is no such loss hole at the outside midplane in any reasonable energy range due to high effective pitch angle collisionality. The only relevant non-ambipolar transport occurs in the X-region as discussed here. The scaling rules for the pedestal width and H-mode power threshold from X-transport, and the effect of neutrals are currently being investigated.

This work is supported by the U.S. DOE and Korea Basic Science Institute.

References

[1] CHANG, C.S., ITER Expert Group Meeting, April, 14-16, 1999, Garching, Germany.
[2] SHAING, K.C., and CRUME, E.C. JR, Phys. Rev. Lett. **63** (1989) 2369.
[3] CARLSTROM, T., ITER Expert Group Meeting, April, 1999, Garching, Germany.
[4] ERIKSSON, L-G, et al, Plasma Phys. Control. Fusion **39** (1997) 27.
[5] CHANKIN, A.V., McCRACKEN, G.M., Nucl. Fusion **33**, (1993) 1459.